

The Global Earthquake Activity Rate (GEAR) forecast test

*David D Jackson¹, Peter Bird¹, Yan Y Kagan¹, Corne Kreemer², Ross Stein³

1.University of California Los Angeles, 2.University of Nevada Reno, 3.Temblor.net

We present a global seismicity reference model based on uniform global datasets, transparently merging the best features of competing approaches and resulting in a testable product. In the past, two approaches to forecasting shallow seismicity have had comparable success. The tectonic method is based on maps of deforming regions and/or active faults, with some empirical calibration of seismic coupling. This captures the distribution of energy sources and may provide good forecasts for very long time windows. The smoothed seismicity approach applies optimized smoothing to cataloged earthquakes. This captures triggering, including ongoing aftershock sequences, and may work best on short to intermediate timescales. Here we combine a leading global forecast of each type using several kinds of combination: linear, log-linear, and an envelope method. We test the success of each parent and hybrid forecast in an 8-year retrospective test by information score, area skill score, and spatial-likelihood metrics that are all roughly independent of total earthquake rate. In this 2005-2012 test, the most successful hybrid model is the log-linear mixture of 60% seismicity with 40% tectonics. This hybrid outperforms both parent forecasts. The chance that this improvement results from a temporary random fluctuation is much less than 1%. We also test all models against the analog-instrumental catalog years 1918-1976; the same patterns of hybrid improvement are found. Likelihood scores are generally less than for the more recent catalog, possibly because of limitations in the older data. We compute an update of the preferred hybrid model using all modern catalog years 1977-2013, for future prospective testing. This hybrid model is named Global Earthquake Activity Rate model 1 (GEAR1) and is provided on a $0.1^\circ \times 0.1^\circ$ global grid, for hypocentroid depths up to 70 km, with magnitude bins whose centers range from 6.0 to 9.0 in steps of 0.10. Comparing our GEAR1 forecast to the recent fault-based UCERF3 long-term forecast in California, we find that both predict the same total earthquake rates (within 4%) at each of two thresholds, but that the map patterns of the GEAR1 forecast most strongly resemble the maps of UCERF3 after spatial smoothing with characteristic distances of 25-30 km has been applied to UCERF3.

Keywords: earthquake, forecast, global, test

Hybrid Models and Time-dependent Hazard in New Zealand

*Matt Gerstenberger¹, David Rhoades, Annemarie Christophersen, David Harte, Bill Fry

1.GNS Science

Recent work in earthquake forecasting in New Zealand has been at the interface of earthquake forecasting (or operational earthquake forecasting) and seismic hazard analysis. One of our aims has been to develop models that can transition from short-term forecasting to the time scales that are required by seismic hazard analysis. As part of this we have been developing hybrid forecast models that utilise alternative data sets to the earthquake catalogue. Recent results have shown significant improvements in forecast skill by including geological information and geodetic strain rate information. Another important challenge has been to develop homogeneous catalogues that allow for consistent forecasting from earthquake rates through to ground-motion prediction equations. We have also been endeavoring to understand the impact of uncertainties (e.g., from the catalogue through to model uncertainty) on the final forecasts. Finally, we will discuss some of the challenges we are currently facing in testing of earthquake forecast models.

Keywords: earthquake forecasting, statistics, seismic hazard

3D spatial models for seismicity beneath Kanto region

*Yosihiko Ogata^{1,2}, Koichi Katsura¹, Hiroshi Tsuruoka², Naoshi Hirata²

1.The Institute of Statistical Mathematics, Research Organization of Information and Systems,
2.Earthquake Research Institute, University of Tokyo

Development of point-process models for the seismicity in 3D space (longitude, latitude and depth) beneath Kanto area down to 100km depth is more required than for seismicity in the rest of the world. This is because the three tectonic plates meet beneath Kanto plain; and interactions among the interplate and intraplate earthquakes are too complex to make detailed analysis and forecasts in 2D space that ignores the depths.

We consider the 3D hierarchical space-time ETAS (epidemic-type aftershock sequence) model. Among the characterizing parameters, the background seismicity rate μ and aftershock productivity K are highly sensitive to the locations, so that these parameters should be location-dependent. Furthermore, the impact of the 2011 Tohoku-Oki earthquake of M9.0 to the seismicity beneath the Kanto region has been so large that we need a space-time function for representing the amount of the induced seismicity beneath Kanto by this giant earthquake. Specifically, we adopt the Omori-Utsu function as the effect of induced earthquakes, started after the occurrence time of the Tohoku-Oki earthquake, where we assume that the aftershock productivity parameter K_{M_0} of the Omori-Utsu function is also location-dependent. For forecasting future large earthquakes, we further need to estimate the location-dependent b -value of the Gutenberg-Richter law.

The spatial variations of the characteristic parameters $\mu(x,y,z)$, $K(x,y,z)$, $K_{M_0}(x,y,z)$ and $b(x,y,z)$ of our model are inverted to visualize the regional changes of the seismic activity. For this objective, we make 3D Delaunay tessellation of the Kanto volume, where every earthquake belongs to vertices of a tetrahedron. Each of the above mentioned parameter function is a 3-dimensional piecewise linear function defined by the values at the four Delaunay tetrahedral vertices.

The estimates of the focal parameter functions are obtained by an optimal trade-off between the goodness of fit to the earthquake data and the smoothness constraints (or roughness penalties) of the variations of parameter values. Strengths of the constraints or the penalties to respective parameter functions can be simultaneously adjusted from the data by means of an empirical Bayesian method using the Akaike's Bayesian information criterion (ABIC).

Keywords: ABIC, aftershock productivity, background seismicity rate, b -values, Delaunay function, Omori-Utsu function for induced seismicity

Optimized physics-based earthquake forecasts for inland Japan

*Margarita Segkou¹, Jiancang Zhuang²

1.BGS, 2.ISM

We focus on the stress recovery processes after the $M=9.0$ Tohoku mega-earthquake and how the above influences the earthquake probabilities in active faults of inland Japan. Recent studies present evidence about rapid stress recovery near the trench but as anticipated by rate-and-state friction law, returning to pre-Tohoku "normal" seismicity levels for the active faults in inland Japan is a slower process. We perform a retrospective forecast spanning 10 years (2004-2014) in the Niigata prefecture (mid-west Japan) using physics-based modeling, combining rate-and-state law and Coulomb stress changes, to study earthquake-triggering mechanisms. The key element of our innovation lies in the development of 429 forecast models, as a result of a stochastic optimization within short-time frames (10 days), in order to access the variability of fault constitutive parameters. The aforementioned optimized forecast then competes with a benchmark statistical/empirical Epidemic-Type Aftershock Sequence (ETAS) model already submitted in CSEP-Japan. The testing period starts with the $M=6.8$ 2004 Chuetsu mainshock and ends on December 2014, approximately 9 months after the $M=6.7$ post-Tohoku mid-Niigata on April 12th, 2011. Our physics-based optimization goes hand in hand with uncertainty consideration related with the estimation of static stress changes (geometry of active faults, receiver depth, effective friction coefficient) following the $M=6.8$ Chuetsu mainshock and important triggered events at the near source are, the 2007 $M=6.7$ Chuetsu-Oki and the $M=6.2$ post-Tohoku event. The forecasts are evaluated for their predictability, spatial consistency and relative information gain through log-statistics by considering the statistical model as reference. We find that: (1) best-fit solutions correspond to stressing rates between 0.01 and 0.8 bar/yr immediately after the aforementioned mainshocks and (2) $\Delta\sigma$ values vary between 0.1 and 2.0, for the few first days following the post-Tohoku and Chuetsu events.

Keywords: physics-based forecasting, stress changes, post-Tohoku recovery

Resolving Stress Singularities: a Retrospective Japan Rate-and-State Earthquake Forecast

*Anne Elizabeth Strader¹, Yosihiko Ogata^{3,2}, Naoshi Hirata², Hiroshi Tsuruoka², Danijel Schorlemmer¹

1.GFZ Potsdam, 2.ERI, The University of Tokyo, 3.The Institute of Statistical Mathematics

Retrospective evaluations of rate-and-state Coulomb stress transfer have shown consistent associations between increased Coulomb stress and seismicity rates. However, stress singularities occurring at the ends of fault dislocation patches tend to provide an unrealistic calculated stress field near active faults, where most earthquakes occur. The effects of such stress calculation artefacts

may be mitigated through implementation of an inverse rate-and-state model, where seismicity rate variations are inverted to obtain Coulomb stress steps over time. The resulting stress variations, from which expected seismicity rates are derived, show potential near the Tohoku rupture plane in a short-term prospective Japan forecast due to low magnitude completeness thresholds, which allow for comprehensive delineation of the Coulomb stress field. An additional advantage of the stress inversion model is that it does not require receiver plane orientations or focal mechanisms, which add uncertainty to the calculated stress field and are not always available, limiting the reliability

of applying the forward model in a global earthquake forecast. We retrospectively test our forecast within all Japan CSEP (Collaboratory for the Study of Earthquake Predictability) testing regions, just after the 2011 Tohoku earthquake. To determine whether the observed seismicity rate variations are sufficient to define Coulomb stress field variations, we combine our forecast with ETAS forecasts currently being tested in the Japan CSEP testing center. At the 95% significance level, the rate-and-state forecast displays potential in defining the magnitude distribution of future earth-

quakes, but does not yet reliably constrain the number, or the spatial distribution of earthquakes away from the mainshock, indicating that the inverse forecast may be most effectively applied in an ensemble earthquake forecast model, where it contributes more to forecasted seismicity rates near areas with recent seismicity.

Keywords: forecast, seismology, Coulomb stress

Impact of automatic catalog quality on real-time aftershock forecasting

*Takahiro Omi¹, Yosihiko Ogata^{2,3}, Katsuhiko Shiomi⁴, Bogdan Enescu^{2,5}, Kaoru Sawazaki⁴, Kazuyuki Aihara¹

1.Institute of Industrial Science, the University of Tokyo, 2.The Institute of Statistical Mathematics, 3.Earthquake Research Institute, University of Tokyo, 4.National Research Institute for Earth Science and Disaster Prevention, 5.Faculty of Life and Environmental Sciences, University of Tsukuba

A hypocenter catalog is the main input for earthquake forecasting. Thus the quality of the catalog may have a considerable impact on the forecasting performance. This issue is important especially for aftershock forecasting because the short-term forecast is prepared based on the hypocenter catalog available in real-time during occurrences of aftershocks, but its quality is generally low as compared to the final version of the edited catalog. For example, many aftershocks including even moderate ones in the first few hours after a main shock are missing in real-time data. Here we are concerned with automatically determined hypocenters without any manual amendments, and we examine how the raw quality of the real-time data affects the performances of aftershock forecasting. In this study we examine the automatic hypocenter catalog of the High Sensitivity Seismograph Network (Hi-net [1]), and conduct forecast experiments of inland aftershock sequences in Japan. We compare forecasting performances between this Hi-net automatic catalog and the JMA revised catalog [2]. We also consider several automatically modified versions of the Hi-net catalog, and examine what kind of factors in the raw catalog are important for improving the forecasting performance.

[1] Okada, Y. et al. (2004), Recent progress of seismic observation networks in Japan -Hi-net, F-net, K-NET and KiK-net-. Earth, Planets and Space 56, 15-28.

[2] T. Omi, Y. Ogata, K. Shiomi, B. Enescu, K. Sawazaki, K. Aihara, "Automatic aftershock forecasting: A forecast test of aftershocks using the real-time data in Japan"
" (in preparation)

Keywords: aftershock, probabilistic forecasting, real-time data

Universal slip statistics: from nanopillars to earthquakes

*Dahmen A Karin¹, Danijel Schorlemmer²

1.Department of Physics, University of Illinois at Urbana Champaign, 2.German Research Centre for Geosciences, Telegrafenberg, 14473 Potsdam, Germany

The deformation of many solid materials is not continuous, but discrete and jerky, with sudden, intermittent slips, similar to earthquakes. We discuss a simple model that predicts that the statistical distributions of the slips should be universal, i.e. they should be the same for many different materials, spanning a wide range of scales, from nanometer-sized crystalline pillars to earthquake faults that are a hundred kilometers long. We show a comparison of the model predictions to recent experiments on many different materials, ranging from nanocrystals, to bulk metallic glasses, to granular materials, to earthquakes and find good agreement with the model predictions. Tools from the theory of phase transition, such as the renormalization group can be used to explain the wide applicability of the simple model. The study provides intuition and a unified framework to understand the fundamental properties of shear-induced deformation in systems ranging from nanocrystals to earthquakes. It also provides many new predictions for future experiments, observations, and simulations. The results can be used for materials testing, evaluation, and hazard prevention.

Reference:

Jonathan T. Uhl, Shivesh Pathak, Danijel Schorlemmer, Xin Liu, Ryan Swindeman, Braden A.W. Brinkman,, Michael LeBlanc, Georgios Tsekenis, Nir Friedman, Robert Behringer, Dmitry Denisov, Peter Schall, Xiaojun Gu, Wendelin J. Wright, Todd Hufnagel, Andrew Jennings, Julia R. Greer, P.K. Liaw, Thorsten Becker, Georg Dresen, and Karin A. Dahmen, Universal Quake Statistics: From Compressed Nanocrystals to Earthquakes, Scientific Reports 5, 16493 (2015)

Keywords: Earthquakes, Statistics, Universality, Seismology, Experiments, Scaling

Evolution of earthquake rupture potential along the Pacific Plate off Japan, inferred from seismicity

Thessa Tormann¹, Stefan Wiemer¹, *Bogdan Enescu^{2,3}, Jochen Woessner⁴

1.ETH Zurich, Switzerland, 2.University of Tsukuba, Japan, 3.Institute of Statistical Mathematics, Tokyo, Japan, 4.Risk Management Solutions Inc., Zurich, Switzerland

One of the major unresolved questions in Seismology is the evolution in time and space of the earthquake rupture potential and thus time-dependent hazard along active faults. What happens after a major event: is the potential for further large events reduced as predicted from elastic rebound, or increased as proposed by current-state short-term clustering models? How does the rupture potential distribute in space, i.e. does it reveal imprints of stress transfer?

Based on the rich earthquake record along the Pacific Plate off Japan we investigate what information on spatial distributions and temporal changes of normalized rupture potential (*NRP*) for different magnitudes can be derived from time-varying, local statistical characteristics of well and frequently observed small-to-moderate seismicity. The *NRP* is obtained from the frequency-magnitude distribution of sampled earthquakes, specifically from the slope (*b*-value) and *y*-intercept (*a*-value) of this distribution, in a log-linear plot. The *b*-values describe the relative frequency of large versus small earthquakes, while *a*-values express the seismic activity during the observation period (in this study, the *a*-values are annualized and distance-weighted, i.e. we consider the relative earthquake-grid-point distances, with close-by events gaining higher weights than more distant events). We analyze the seismicity from 1998 ~ 2015, including the massive 2011 M9 Tohoku-oki earthquake and its aftermath.

Seismicity records show strong spatio-temporal variability in both activity rates and size distribution. We show first (Tormann et al., 2015) that the size distribution of earthquakes has significantly changed before (increased fraction of larger magnitudes -relatively small *b*-values) and after that mainshock (increased fraction of smaller magnitudes -relatively large *b*-values); these changes are particularly stronger in areas of highest Tohoku-oki coseismic slip. Remarkably, a rapid recovery of this effect is observed within only few years.

We then combine this significant temporal variability in earthquake size distributions (*b*-values) with local activity rates (*a*-values) and infer the evolution of *NRP* distributions. We study complex spatial patterns and how they evolve with time, focusing on the detailed temporal characteristics in a simplified spatial selection, i.e. inside and outside the high slip zone of the M9 earthquake. We resolve an immediate and strong *NRP* increase for large events prior to the Tohoku-oki event in the subsequent high slip patch and a very rapid decrease inside this high-stress-release area, coupled with a lasting increase of *NRP* in the immediate surroundings. Even in the center of the Tohoku rupture, the *NRP* for large magnitudes has not dropped below long-term average values and is now not significantly different from conditions a decade before the M9 event.

Keywords: Tohoku-oki earthquake, seismic hazard, subduction zone seismicity

ISC Data for Earthquake Statistics

*Dmitry Storchak¹, Domenico Di Giacomo¹, James Harris¹

1. International Seismological Centre

The International Seismological Centre (ISC) is charged with production of the ISC Bulletin –the definitive summary of the global seismicity covering the entire period of instrumental recordings between 1904 and 2016. It is based on the reviewed seismic bulletin reports from over 130 seismic networks worldwide and includes a total of 5.8 million seismic events with 1.9 millions of them reviewed by the ISC analysts. The main purpose of this huge dataset is to include as many seismic events around the globe as possible to provide the most complete and comprehensive list of earthquakes and other seismic events in a homogeneous way. In fact, there are considerable temporal and region-to-region variations in the magnitude completeness and hypocentre location accuracy of reports from local and regional seismic networks and observatories. These variations are dictated by the distribution and quality of local seismic networks, waveform processing procedures as well as administrative and political decisions that control reporting bulletin data to the ISC. The content of local bulletin reports have also changed dramatically through the period of instrumental recordings thus affecting the content of the ISC Bulletin as a whole. Statistical studies of seismicity patterns, b-value, earthquake rate are also subject to an accurate identification of anthropogenic events or events caused by anthropogenic activities. These studies often require the removal of aftershocks series. This presentation lays out major principles of building the ISC Bulletin, describes the complexity of event information, and provides recommendations for practical use of the enclosed information.

In addition to the Bulletin as its flagship product, the ISC is maintaining a set of specialized products that both narrow down and extend the information from the ISC Bulletin to serve the purpose of specific groups of geoscientists. Thus we prepared and continue extending the ISC-GEM Global Instrumental Earthquake Catalogue widely used for estimation of global and regional earthquake hazard. The ISC-EHB dataset is maintained for users interested in less complete list of events with considerably higher accuracy of event epicenter and depth determination. It is used in global and regional studies of tectonics, surface geology and inner structure of the Earth. Other datasets include the GT bulletin, CTBTO Link, Event Bibliography and Seismological Contacts.

Keywords: earthquake, global, bulletin

Underestimate of the size of microearthquakes by the JMA magnitude scale and its influence to earthquake statistics

*Takahiko Uchide¹, Kazutoshi Imanishi¹

1. Research Institute of Earthquake and Volcano Geology, Geological Survey of Japan, National Institute of Advanced Industrial Science and Technology (AIST)

Earthquake statistics needs parameterized information on earthquakes. One of such parameters is the magnitude. The local magnitude scales, such as the JMA magnitude (M_j), based on amplitudes of seismograms are easy to estimate and therefore usually included in earthquake catalogs. The moment magnitude (M_w) is based on the physical source parameter, seismic moment, however needs much effort for the estimation especially for microearthquakes. Though the consistency between M_j and M_w is guaranteed for the medium earthquakes, we need to check that for microearthquakes.

As for use of earthquake catalogs, we should know the completeness magnitude above which catalog is complete. A type of it is M_c defined as a magnitude where magnitude-frequency distribution starts deviating from the Gutenberg-Richter's (GR) law. Another one is based on earthquake detectability. Schorlemmer and Woessner [2008] proposed M_p based on the detectability inferred from the pick information. They showed the Californian case that M_p is smaller than M_c , which indicates the breakdown of the GR law. It is important to confirm if the breakdown really occurs. Our study investigates if the discrepancies are also seen in case of M_w .

M_w Estimation for Microearthquakes

We stably estimate seismic moment of microearthquakes based on moment ratios to nearby small earthquakes whose seismic moments are available in the NIED MT catalog, by a multiple spectral ratio analysis [Uchide and Imanishi, under review]. Applying this method to earthquakes in Fukushima Hamadori and northern Ibaraki prefecture areas, eventually we obtained the seismic moments of a total of 19140 earthquakes (M_j 0.4 - 3.8). The striking result of this study is that the change in slopes of the M_j - M_w curve: 1 and 0.5 at higher and lower magnitudes, respectively (see Figure). The discrepancies between M_j and M_w are significant for microearthquakes, suggesting that M_j underestimates the sizes of microearthquakes.

Completeness Magnitudes and b-values

The result above must affect earthquake statistics. Here we study M_c and b-value of the GR law. Following Ogata and Katsura [1993], we assume the earthquake detectability as the cumulative normal distribution with a mean, μ , and a standard deviation, σ , and estimate the GR parameters (a and b) together with μ and σ . We define $M_c = \mu + 2.33\sigma$ where the detection rate is 99%. Applying this method to the monthly seismicity data in the study area, we found that the M_c for M_w is lower than that for M_j converted into M_w , however still larger than M_p converted into M_w . This may be due to the breakdown of the GR law for microearthquakes, though another possibility is that the incompleteness of earthquake catalog overestimates the detectability, resulting the underestimate of M_p .

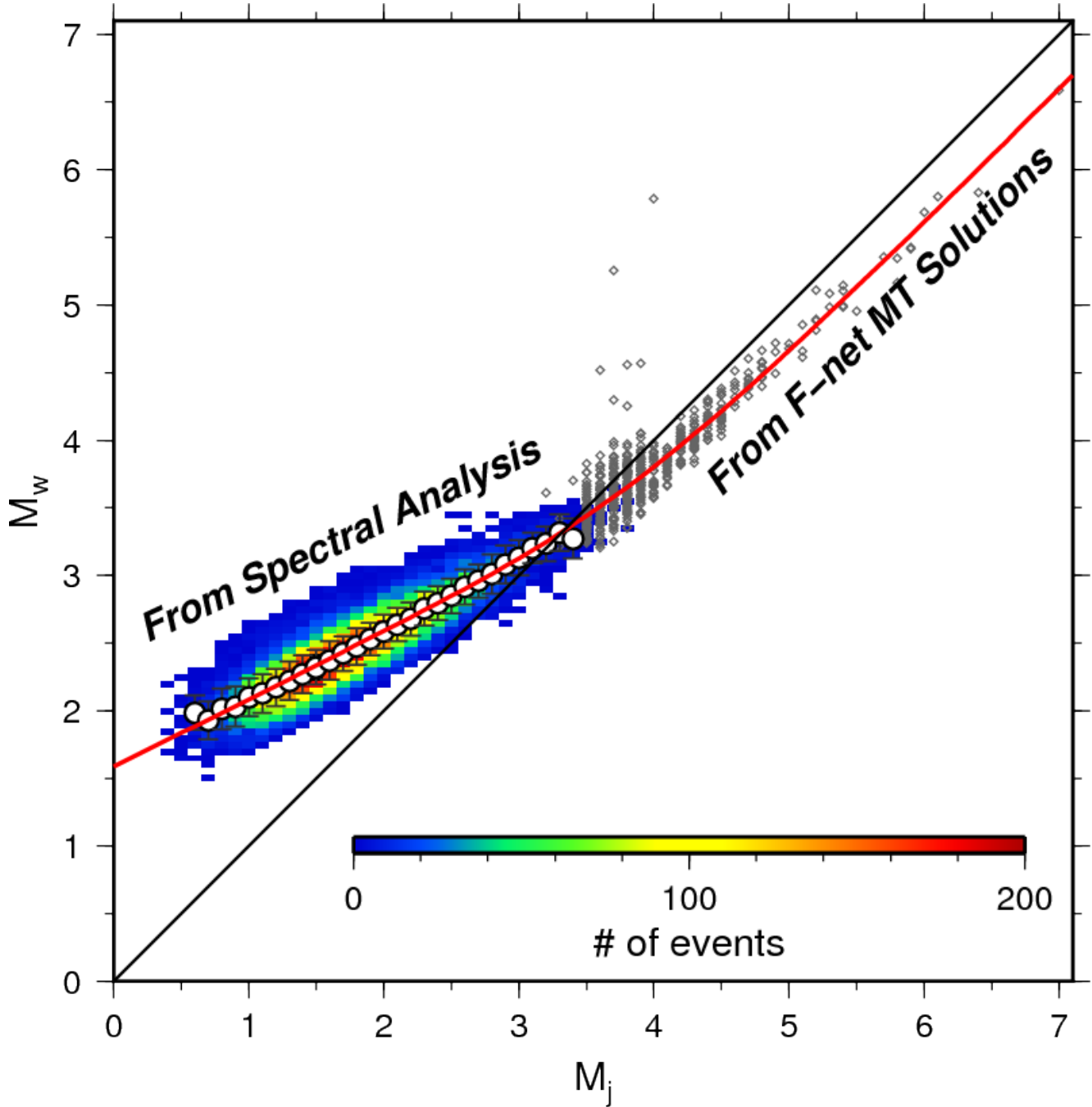
b-values for M_w (b_w) are systematically larger than those for M_j (b_j). The temporal trends for b_w and b_j are similar to each other. When b_j increases, b_w also increases. This does not affect discussions inferred from the qualitative temporal change in b-values [e.g., Nanjo et al., 2012]. b_w is often larger than 1.5, indicating that the moment release is dominantly done by smaller earthquakes.

Acknowledgement

We used the JMA Unified Earthquake Catalog, seismograms from NIED Hi-net and the NIED moment tensor catalog.

Figure: Comparison between M_j and M_w inferred from the multiple spectral ratio analyses (color image for the distribution and circles for the median M_w) and the NIED MT solutions.

Keywords: Earthquake statistics, JMA magnitude, Moment magnitude, Spectral analysis, Completeness magnitude, b-value



Assessment and optimization of the potential earthquake precursory information in ULF magnetic data registered at Kanto, Japan during 2000 -2010

*Peng Han^{1,2}, Katsumi Hattori¹, Jiancang Zhuang²

1.Graduate School of Science, Chiba University, Chiba, Japan, 2.Institute of Statistical Mathematics, Tokyo, Japan

In order to clarify the ULF seismo-magnetic phenomena, a sensitive geomagnetic network has been installed at Kanto, Japan since 2000. In previous study, we have verified the correlation between ULF magnetic anomalies and local sizeable earthquakes by both case and statistical studies. In this paper, we use the Molchan's error diagram to evaluate the potential earthquake precursory information in the magnetic data registered at Kanto, Japan during 2000 -2010. The results show that the earthquake predictions based on magnetic anomalies are clearly better than those based on random guess, which indicates the magnetic data contain potential useful prediction information. Further investigations suggest that the prediction efficiency depends on the distance (R) and the size of the target earthquake events (E_s). Finally, we introduce the probability gain (PG') and the probability difference (D') to explore the optimal prediction parameters for a given ULF magnetic station. For Seikoshi (SKS) station in Izu, optimal R and E_s are about 100 km and $10^{8.75}$, respectively; and for Kiyosumi (KYS) station in Boso, they are about 180 km and $10^{8.75}$, respectively.

Keywords: earthquake precursory information, Molchan's error diagram, statistical analysis, parameter optimization , ULF magnetic data

Prospective validation of physical-based precursors and their potential for short-term earthquake forecasting. Case study for Japan 2014-2016

*Dimitar Ouzounov¹, Katsumi Hattori²

1.Center of Excellence in Earth Systems Modeling & Observations (CEESMO) , Schmid College of Science & Technology Chapman University, Orange, California, USA, 2.Department of Earth Sciences, Chiba University, Chiba, Japan

We are presenting a prospective validation of short-term pre-earthquake phenomena preceding major earthquakes. Our challenge question is: "Whether such physical-based signals are significant and could be used for early warning of large earthquakes?" To address this question we have started continuous validation of atmospheric signals in retrospective/ prospective modes over Japan. Our approach is based on multidisciplinary analysis of several physical and environmental parameters (Satellite transient infrared radiation (STIR), electron concentration in the ionosphere (GPS/TEC), radon/ion activities, air temperature and seismicity patterns) that were found to be associated with earthquakes. The science rationale for multidisciplinary analysis is based on concept Lithosphere-Atmosphere-Ionosphere Coupling (LAIC) (Pulinets and Ouzounov, 2011]), which explains the synergy of different processes and anomalous variations, usually named short-term pre-earthquake anomalies.

Our validation processes consist in two steps: (1) A continuous retrospective analysis performed over two different regions with high seismicity- Taiwan and Japan for 2003-2011 (2) Prospective testing with potential for M6.5+ events Japan for 2014-2015 period. The test results suggest appearance of physical pre-earthquake anomalies, one to several days in advance to major events, including the largest earthquakes - M7.8 of 30 May 2015 and all other M6.5+ for that period. The false alarm ratio for the testing period has shown false positives less than 20%. Our initial prospective tests show that multi-parameter analysis could reveal short-term pre-earthquake anomalies prior to the largest earthquakes in Japan.

Keywords: earthquake precursor, forecasting, early warning system